A Near-Optimal UAV-Aided Radio Coverage Strategy for Dense Urban Areas

Xiaowei Li, Haipeng Yao, *Member, IEEE,* Jingjing Wang, *Member, IEEE,*
Xiaobin Xu, Chunxiao Jiang, *Senior Member, IEEE,* and Lajos Hanzo, *Fellow, IEEE*

Abstract—Unmanned aerial vehicles (UAVs) may be used for providing seamless network coverage in urban areas for improving the performance of conventional cellular networks. Given the predominantly line-of-sight (LOS) channel of drones, UAV-aided seamless coverage becomes particularly beneficial in case of emergency situations. However, a single UAV having a limited cruising capability is unable to provide seamless long-term coverage, multiple drones relying on sophisticated recharging and reshuffling schemes are necessary. In this context, both the positioning and the flight strategy directly affect the efficiency of the system. Hence, we first introduce a novel UAV energy consumption model, based on which an energy-efficiency based objective function is derived. Secondly, we propose an energy-efficient rechargeable UAV deployment strategy optimized under a seamless coverage constraint. Explicitly, a two-stage joint optimization algorithm is conceived for solving both the optimal UAV deployment as well as the cyclic UAV recharging and reshuffling strategy (CRRS). Our simulation results quantify the efficiency of our proposed algorithm.

Index Terms—Unmanned aerial vehicle (UAV), seamless coverage, cyclic recharging and reshuffling strategy (CRRS).

I. INTRODUCTION

GIVEN their low cost and high flexibility, unmanned aerial vehicles (UAVs) may find application both in military and in civilian scenarios for supporting seamless information services [1]. More explicitly, UAVs can be viewed as 'airborne access points' (AAPs), which are capable of providing high-quality line-of-sight (LOS) links upon avoiding blockage by tall buildings and trees on the ground [2]–[5]. Furthermore, UAV-assisted on-demand communication may be the only viable technique of supporting seamless broadband information coverage in the context of disasters, when the terrestrial infrastructure breaks down. However, the energy constraint of a single drone limits both its cruising and hovering duration, but fortunately the cooperation of networked UAVs is capable of improving the situation [6], [7]. Hence, how to design an efficient UAV deployment strategy and cruising route for supporting seamless coverage becomes a crucial problem.

Energy-efficient UAV assisted information services have been widely investigated in the literature. Alzenad *et al.* [8] explored an energy-efficient 3D UAV placement scheme for maximizing the number of users that can be served at the minimum transmit power. Mozaffari *et al.* [9] proposed a beneficial resource allocation scheme by striking a trade-off between the communication capability and the UAV's hovering duration. However, the authors of [8] and [9] only aimed for optimizing the transmit power. Given the fact that the energy consumed by the propulsion of drones is much higher than that consumed by communication, Lu *et al.* [10] focused their attention both on the on-board circuit power and on the propulsion power requirements for the sake of minimizing the frequency of the UAV's battery charging operation. Furthermore, the authors of both [11] and [12] considered the UAV's propulsion power in the context of UAV-to-ground communications. By contrast, the authors of both [13] and [14] aimed for finding the energy-efficient flight path of UAVs under the condition of sweeping through all IoT nodes, since communications in IoT systems tend to be delay-tolerant [15]. Even though these contributions have indeed considered the propulsion power of drones, the limited flight duration may also limit the practicability of drones in supporting seamless and long-term network coverage. Arranging for the cooperation of multiple rechargeable UAVs may be the only viable way of providing seamless long-term communication services to users, where each target point has at least one drone at any moment of service provision.

In this paper, we consider a swarm of rechargeable UAVs providing seamless long-term coverage. Given the energy constraint of UAVs, improving the energy efficiency as well as maintaining seamless coverage poses a critical challenge. To address this challenge, we consider an energy-efficient UAV-aided seamless information infrastructure conceived for a dense urban area relying on small rechargeable drones, where the drones having a low battery level should return to the charging station for replenishing their energy. At the same time, the drones having high-battery level take over the provision of information services at the target location. Our new contributions are summarized as follows:

- To the best of our knowledge, this is the first study of an energy-efficient UAV-aided seamless long-term infor-

X. Li and X. Xu are with the Beijing Advanced Innovation Center for Future Internet Technology, Beijing University of Technology, Beijing, China, 100124, E-mail: lixiaowei_bjut@163.com, doublexb@163.com.

H. Yao is with the State Key Laboratory of Networking and Switching Technology, Beijing University of Posts and Telecommunications, Beijing, China, 100876, E-mail: yaohaipeng@bupt.edu.cn.

J. Wang is with the Department of Electronic Engineering, Tsinghua University, Beijing, China, 100084. E-mail: chinaeephd@gmail.com.

C. Jiang is with the Tsinghua Space Center, Tsinghua University, Beijing, China, 100084. E-mail: jchx@tsinghua.edu.cn.

L. Hanzo is with the School of Electronics and Computer Science, University of Southampton, Southampton, SO17 1BJ, UK. E-mail: lh@ecs.soton.ac.uk.

mation coverage infrastructure relying on a beneficially designed UAV deployment strategy, which specifically considers the propulsion power and recharging strategy of small drones.

- We simplify the energy-efficient information coverage problem into a generalized assignment problem. Moreover, a two-stage joint UAV deployment as well as cyclic UAV recharging and reshuffling optimization algorithm is proposed, which is then solved based on an efficient particle swarm optimization (PSO) algorithm.
- The performance of our proposed two-stage joint optimization algorithm is characterized by extensive simulations.

The rest of this paper is organized as follows. Section II surveys the prior art on the subject of the paper. In Section III, the channel model as well as the cyclic recharging and reshuffling strategy (CRRS) is defined, and then the energy efficient CRRS problem is formulated. Section IV introduces our PSO-based two-stage algorithm and analyzes its complexity. In Section V, we present our simulation results. Finally, the paper is concluded in Section VI.

II. RELATED WORKS

As a benefit of the UAVs' flexibility, UAV-assisted communications may find applications in diverse scenarios [16], [17]. One of the aspects is the provision of long-lasting seamless *UAV-aided coverage* [18]–[27]. Naturally, this ambitions goal is assisted by *UAV-aided relaying* [28]–[30], where UAVs act as relays for the sake of enhancing the connectivity of two or more distant nodes. This is achieved by taking advantage of the high probability of LOS channels as a benefit of their high altitude. The third application is *UAV-aided information dissemination and data collection* [13], [14], [31], [32], where the UAV collects or broadcasts non-realtime sensor data to distributed nodes, when the UAV scans the target area.

As for the UAV-aided seamless coverage, several state-of-the-art studies have been disseminated [18]–[27]. To elaborate, Hourani *et al.* [18] analyzed the altitude of the UAV with the intention of maximizing the coverage quality/area in urban environments. Their results showed that the optimal altitude was determined by the maximum allowed path-loss as well as by the statistical parameters of the target environment. Mozaffari *et al.* [19] studied the 3D deployment of two UAVs for maximizing the coverage quality/area and minimizing the transmit power considering both interference-free and interference-infested scenarios. By contrast, Alzenad *et al.* [20] focused their attention on the 3D UAV placement for maximizing the number of users having different QoS requirements. Moreover, Yaliniz *et al.* [21] investigated the optimal UAV placement mainly for maximizing the revenue of the network. Tao *et al.* [22] addressed the problem of capacity enhancement using UAVs in tele-traffic hot-spots by relying on an analytical ergodic capacity model., The authors of [23]–[25] focused their attention on conceiving efficient UAV deployment algorithms for covering the target area. Furthermore, UAV-aided communication systems can also co-exist with other systems. In this spirit, Mozaffari *et al.* [26]

considered underlaid device-to-device (D2D) communication within a UAVs' coverage area, where they studied the optimal UAV deployment with the objective of maximizing the number of D2D user supported both by static and by mobile UAV. Lyu *et al.* [27] analyzed the coexistence of the UAV as an arial BS and of a ground BS. Explicitly, they jointly considered the optimization of the UAVs' flight trajectory, resource allocation and user assignment.

In carefully considering the UAV's limited flight duration, maximizing the energy efficiency is critical. The authors of [8] focussed their attention on the optimal 3D deployment of UAVs for minimizing the transmit power by formulating the deployment problem as a circle placement problem. By contrast, Wang *et al.* [33] considered both hotspot and average tele-traffic scenarios. Yu *et al.* [34] aimed for minimizing the transmit power of mobile devices by dynamically deploying UAVs upon additionally taking into account the mobility of devices on the ground. However, the propulsion power consumption of UAVs is much higher than their transmit power consumption, hence the former determines the service duration of UAV. Li *et al.* [28] investigated the specific choice of the optimal cooperative UAV-aided relaying scheme for the sake of maximizing the network life time and at the same time guaranteeing the bit error rate (BER) requirement by carefully balancing the energy consumption of UAVs. Zhang *et al.* [29] aimed for striking a trade-off between the bandwidth efficiency and energy efficiency by appropriately adjusting the time allocation as well as flying speed and trajectory. Moreover, Angelo *et al.* [35] investigated how to prolong the network life time for various target area coverage ratios by considering the recharging operation. As a further development, Hua *et al.* [13] proposed an optimal communication scheme by jointly considering the user schedule, UAV trajectory and power allocation for minimizing the power consumption of UAVs. Franco *et al.* [14] focused their attention on finding energy efficient flight paths for scanning all ground users in practical non-regular coverage area. Mozaffari *et al.* [31] investigated the optimal UAV movement for minimizing the uplink transmit power of IoT nodes in an IoT network, while jointly considering the device association, device power control and UAV position. Relying on the specific design of fixed-wing UAVs, a trade-off was struck between the transmission energy of IoT nodes and the propulsion energy of the UAV by Yang *et al.* [12]. However, in contrast to the IoT scenario, the provision of seamless UAV-aided coverage for users on the ground requires access to at least one UAV at any time.

III. SYSTEM MODEL AND PROBLEM FORMULATION

As shown in Fig. 1, we consider a multi-UAV scenario, where M drones serve as base stations for providing information services for users on the ground. All the drones are capable of operating in both cruising and hovering modes at the same altitude H. Each UAV is equipped with a rechargeable battery and can serve the users within a circle having the radius of R. The capacity of each UAV's battery is denoted by W. In our model, we assume that there are a total of N target service locations for the hovering drones,
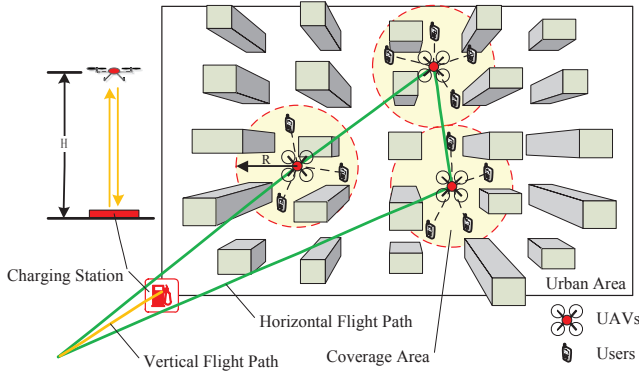
Fig. 1. UAV aided seamless coverage.

TABLE I
SUMMARY OF NOTATIONS

Symbol	Description
N	Total number of target service locations
H	Flight altitude of UAVs
R	Coverage radius of the UAV
W	Capacity of the UAV's battery
M	Total required number of UAVs
J	Total required number of flight circles
M_j	Required number of UAVs in the j-th flight circle
N_j	Number of target service locations in the j-th flight circle
η_{los}, η_{nlos}	The attenuation factors corresponding to the LOS and NLOS UAV-user channel
a, b	Environment-specific coefficients
P_{tr}	Transmit power of the UAV
p_{los}	Probability of LOS channel in the UAV-user links
$\overline{L}_m(r)$	Average path loss of the UAV-user link for the users that are r far from the m-th UAV
$C_n(R)$	The capacity supported by the UAV located at the n-th target location with the coverage radius R
T_{charge}	Charging duration of the UAV at the charging station
T_{home}	The duration that includes the durations of vertical descending, charging and vertical ascending over the charging station
T_j^h	Hovering duration of the UAV at each target location in the j-th flight circle
T_j^d	Total discharging duration of the UAV in the j-th flight circle
T_j	Charging-and-discharging period of the UAV in the j-th flight circle
D_j	Total path length of the j-th flight circle
$P_j(t)$	Instantaneous power at time t of the UAV in the j-th flight circle
P_h	Hovering power of the UAV
P_t, V_t	Traveling power and traveling speed of the UAV
P_a, V_a	Ascending power and ascending speed of the UAV
P_d, V_d	Descending power and descending speed of the UAV

and UAVs provide information services while hovering at one of the target locations. They can also be equipped with a small balloon inflated by a cartridge for saving energy when hovering or for preventing crashing owing to sudden loss of battery power. For the sake of providing seamless information coverage for ground users, a cyclic recharging and reshuffling strategy (CRRS) is conceived, where the drones having a high-battery level replace the low-battery drones in the provision of coverage at the target location. To achieve this, the UAVs visit all or some of the target service locations during their charging-discharging cycles.

In our model, a single fixed charging station is considered, which is located at the bottom left corner of Fig. 1. We assume that each UAV has the same charging duration T_{charge}. Moreover, ground users are capable of accessing the UAV via orthogonal frequency division multiplex access (OFDMA), hence we neglect the interference amongst the UAV-user links. The UAVs can cache data in advance, and exchange data through UAV-UAV links, where the UAV-UAV links are modelled as a line-of-sight channel associated with different frequency bands than the UAV-user links. Assuming that the UAV-UAV LOS links have sufficient capacity, we only consider the downlink air-to-ground channel model in the paper.

A. Air-to-Ground Channel Model

In the paper, we focus on the downlink model of UAV-user communications. We consider a pair of air-to-ground communication channels, i.e. the LOS channel and the non-line-of-sight (NLOS) channel. Given a UAV m located at (X_m, Y_m) and a user located at (x, y), the path loss between (X_m, Y_m) and (x, y) can be expressed by [10]:

$$\begin{cases} L_{m,los}(x,y) = \eta_{los}\left(\frac{4\pi f}{c}\right)^2 d_m^2(x,y), & \text{if LOS link,} \\ L_{m,nlos}(x,y) = \eta_{nlos}\left(\frac{4\pi f}{c}\right)^2 d_m^2(x,y), & \text{if NLOS link,} \end{cases}$$
(1)

where η_{los} and η_{nlos} represent the attenuation factors corresponding to the LOS and NLOS link, respectively, while f is the carrier frequency and c denotes the speed of light. Furthermore, $d_m(x,y) = \sqrt{(x-X_m)^2 + (y-Y_m)^2 + H^2}$ is the distance between the UAV m and the user considered. In our paper, the probability of having a LOS UAV-user link can be expressed as:

$$p_{los}(r) = \frac{1}{1 + a\exp(-b[\theta - a])},$$
(2)

where a and b represent environment-specific coefficients [18], while we have $\theta = \frac{180}{\pi}\tanh(H/r)$ and $r = \sqrt{(x-X_m)^2 + (y-Y_m)^2}$. Hence, the probability of a NLOS link obeys $p_{nlos}(r) = 1 - p_{los}(r)$. Therefore, the average path loss can be formulated as:

$$\bar{L}_m(r) = p_{los}L_{m,los} + (1 - p_{los})L_{m,nlos}.$$
(3)

Let the downlink transmit power of each UAV be P_{tr}. Then, upon relying on Shannon's formula, the average capacity of each link can be formulated as:

$$\bar{c}_m(r) = B\log_2\left(1 + \frac{P_{tr}}{\bar{L}_m(r)\sigma^2 B}\right),$$
(4)

where B represents the bandwidth allocated to the user, while σ^2 is the white Gaussian noise variance at the receiver. Given its circular service area with a radius of R, the capacity supported by the UAV m can be calculated as:

$$C_m(R) = \int_0^R \lambda(r)\bar{c}_m(r)dr,$$
(5)

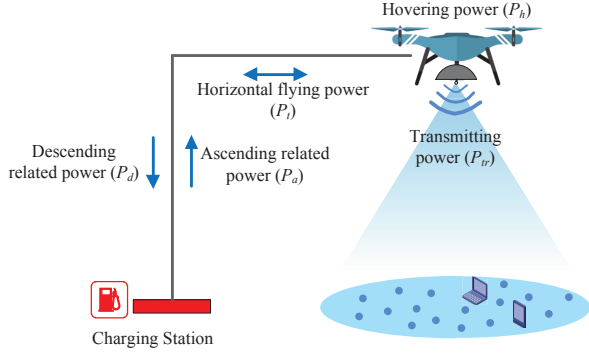where $\lambda(r)$ denotes the user density.

Fig. 2. The power consumption model of a drone.

B. Cyclic Recharging and Reshuffling Strategy for UAVs

The CRRS of UAVs is conceived for providing ground users with seamless information services. However, each drone has to leave its service location for recharging, when its battery level is below the alert level. Meanwhile, another drone should replace the low-battery drone at the target location for supporting uninterrupted service. In this paper, we assume that during a single discharging cycle, a drone cannot visit all the N target locations. Hence, we have a total of J independent flight route circles for covering all the N target locations. In the j-th flight circle, N_j target locations are served by M_j UAVs, and we have $\sum_{j=1}^{J} N_j = N$ as well as $\sum_{j=1}^{J} M_j = M$.

1) UAV Power Model: The power of a multi-rotor UAV has three components [36], i.e. the induced power P_i, the profile power P_p and the parasite power P_{par}. Let mg be the gravity of the UAV, $T = \sqrt{(mg - (c_5(V_{hor}cos\alpha)^2 + c_6T))^2 + (c_4V_{hor}^2)^2}$ be the thrust, V_{vert} and V_{hor} be the vertical speed and horizontal speed. The induced power P_i which produces thrust by propelling air downward can be formulated as [36]:

$$P_i(T, V_{vert}) = k_1 T \left[\frac{V_{vert}}{2} + \sqrt{\left(\frac{V_{vert}}{2}\right)^2 + \frac{T}{k_2^2}} \right]. \quad (6)$$

The profile power P_p overcomes the rotational drag encountered by the rotating propeller blades, which can be expressed by [36]:

$$P_p(T, V_{hor}) = c_2 T^{3/2} + c_3 (V_{hor}cos\alpha)^2 T^{1/2}, \quad (7)$$

where α shows the angle of attack when V_{hor} is not zero. The parasite power P_{par} is used to resist body drag when there is relative translational motion between the vehicle and wind, which can be expressed by [36]:

$$P_{par}(V_{hor}) = c_4 V_{hor}^3. \quad (8)$$

The notations $k_1, k_2, c_2, c_3, c_4, c_5, c_6$ in Eq. (6), Eq. (7) and Eq. (8) represent constant parameters related to the physical properties of the UAV.

For the sake of avoiding collision with buildings, the power consumption model of a drone is illustrated in Fig. 2, i.e. horizontally flying from one target location to the next target location, hovering at one target location for providing services,

vertically descending to the ground at the charging station and vertically ascending to the altitude H, when fully charged. Specifically, we define P_t representing the power required for horizontally flying at a constant speed V_t. From Eq. (6) to Eq. (8), P_t can be derived as [36]:

$$\begin{aligned} P_t(V_t) &= P_i(T, 0) + P_p(T, V_t) + P_{par}(V_t) \\ &= (c_1 + c_2)T^{3/2} + c_3(V_t cos\alpha)^2 T^{1/2} + c_4 V_t^3 \quad (9) \\ &\approx (c_1 + c_2)T^{3/2} + c_4 V_t^3, \end{aligned}$$

where $c_1 = \frac{k_1}{k_2}$. Similarly, the hovering power represented by P_h can be expressed by [36]:

$$P_h = P_i(T, 0) + P_p(T, 0) = (c_1 + c_2)(mg)^{3/2}. \quad (10)$$

Considering a constant ascending speed of V_a and descending speed of V_d, the ascending-related power denoted by P_a and the descending-related power denoted by P_d of the UAV at the charging station can be derived based on Eq. (6), Eq. (7) and Eq. (8), that is [36]:

$$\begin{aligned} P_a(V_a) &= P_i(T, V_a) + P_p(T, 0) \\ &= k_1 mg \left[\frac{V_a}{2} + \sqrt{\left(\frac{V_a}{2}\right)^2 + \frac{mg}{k_2^2}} \right] + c_2(mg)^{3/2}, \end{aligned}$$

$$\quad (11)$$

$$\begin{aligned} P_d(V_d) &= P_i(T, -V_d) + P_p(T, 0) \\ &= k_1 mg \left[\frac{-V_d}{2} + \sqrt{\left(\frac{V_d}{2}\right)^2 + \frac{mg}{k_2^2}} \right] + c_2(mg)^{3/2}. \end{aligned}$$

$$\quad (12)$$

We can see from Eq. (9) to Eq. (12) that P_h, P_t, P_a and P_d are all fixed when given fixed V_t, V_a and V_d. Since the transmit power (normally less than 1W) used for communication is significantly lower than the flight power (normally more than 100W) of a UAV, the transmit power is neglected in the power model. Then, neglecting the acceleration and deceleration process of the UAV, the total energy consumed by a UAV during its j-th flight circle can be approximated by:

$$\int_0^{T_j^d} P_j(t)dt \triangleq \sum_{n=1}^{N_j} P_h T_{j,n}^h + \sum_{k=1}^{N_j+1} P_t \frac{d_{j,k}}{V_t} + P_a \frac{H}{V_a} + P_d \frac{H}{V_d}, \quad (13)$$

where T_j^d is the total discharging duration of the drone in the j-th flight circle, while $T_{j,n}^h$ is its hovering duration at the n-th target location, i.e. its service duration. There are a total of $(N_j + 1)$ flight path segments when the drone visits N_j target locations and the charging station, and $d_{j,k}$ represents the length of the k-th flight path segment. Assuming that the total battery energy of each UAV is W, the energy constraint of a single UAV in the j-th flight circle can be expressed by:

$$\int_0^{T_j^d} P_j(t)dt \leq W, \quad \forall j = 1, 2, ..., J. \quad (14)$$

2) CRRS Constraint: We assume that each UAV has the same energy storage (battery) and can support the same total service duration.

In order to provide seamless coverage for N_j target locations using M_j UAVs in the j-th flight circle, when a UAV leaves
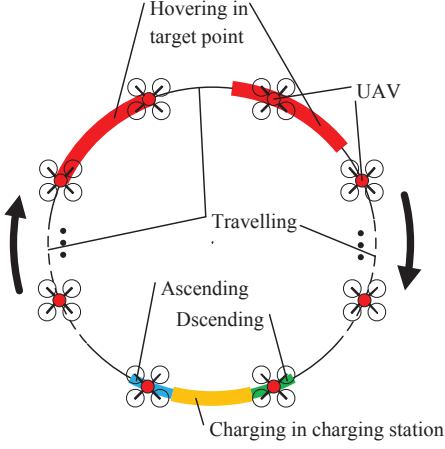
Fig. 3. The CRRS strategy of UAVs.

a target point, an alternative UAV should fly to the related point for replacing the low-energy UAV. Since the flight time interval of UAVs depends on the smallest $T_{j,n}^h$, $T_{j,n}^h$ should have the same value in the j-th flight circle, that is we have $T_{j,n}^h = T_j^h, \forall n = 1, 2, ..., N_j$. Hence, M_j UAVs construct a circular chain relying on the same trajectories as well as on the same service schedule, which is shown in Fig. 3. The arc lengths in Fig. 3 indicate the durations of UAVs in their various states, where the perimeter of the circle shows the UAV's charging-and-discharging period. It is plausible that the time interval between the UAVs should be less than T_j^h for guaranteeing seamless services provision at the target points. Therefore, the total service duration of all M_j reshuffling UAVs should be longer than the total duration of a UAV's charging-and-discharging period. Hence we have:

$$M_j T_j^h \geq \frac{\sum_{k=1}^{N_j+1} d_{j,k}}{V_t} + N_j T_j^h + T_{home}, \quad (15)$$

where $T_{home} \triangleq T_{charge} + H/V_a + H/V_d$, and T_{charge} is the charging duration of each UAV at the charging station. We define $D_j = \sum_{k=1}^{N_j+1} d_{j,k}$, and the service duration T_j^h of a UAV at a specific target location can be formulated by:

$$T_j^h \geq \frac{\frac{D_j}{V_t} + T_{home}}{M_j - N_j}, \quad (16)$$

where we require $M_j > N_j$.

C. Problem Formulation

In this section, first of all, we denote the UAV deployment strategy as A and the UAV CRRS strategy as B. Given a fixed value of N, A represents the strategy conceived for determining the N specific UAV hovering locations, while B represents the policy determining the J flight circles, including the value of N_j and M_j in each flight circle. Let $T_j \triangleq \frac{\sum_{k=1}^{N_j+1} d_{j,k}}{V_t} + N_j T_j^h + T_{home}$ be the charging-and-discharging period of the UAV in the j-th flight circle. In this paper, we assume that only one UAV can provide information services when multiple UAVs overlap in a target location. Hence, from Eq. (15) and Fig. 3, T_j also indicates the total

service duration of M_j UAVs at each target point in the j-th flight circle. Moreover, the system's energy efficiency, where M UAVs serve a total of N target locations relying on J flight circles, can be defined as:

$$\eta(A, B) = \frac{\sum_{j=1}^{J} \sum_{n=1}^{N_j} T_j C_n(R)}{\sum_{j=1}^{J} M_j W}, \quad (17)$$

where $C_n(R)$ is the downlink capacity of the UAV hovering at the n-th target location, which is formulated by Eq. (5). The numerator of Eq. (17) shows the amount of transmitted information, while each UAV completes a charging-and-discharging operation. The denominator of Eq. (17) indicates the total expended energy. Observe from Eq. (17) that the deployment locations directly determine the capacity of UAVs, since the user density in the covered zone directly affects the capacity, but at the same time the overlapping of covered zones potentially reduces the capacity, while users connect the nearest drone. Moreover, in Eq. (16), D_j is jointly determined by the specific deployment locations as well as by the CRRS strategy, and the CRRS strategy in turn also determines N_j. Therefore, the deployment locations and the CRRS strategy jointly determine the number M_j of UAVs required. Hence, strategy A and strategy B jointly affect the system's energy efficiency η. Our objective is to maximize the energy efficiency η. Hence, the joint UAV deployment as well as UAV cyclic recharging and reshuffling optimization problem can be formulated as:

$$P1: \quad \max_{A,B} \quad \eta(A, B)$$

$$\text{s.t.} \quad C1: \int_0^{T_j^d} P_j(t)dt \leq W, \quad \forall j = 1, 2, ..., J,$$

$$C2: M_j T_j^h \geq T_j > 0, \quad \forall j = 1, 2, ..., J, \quad (18)$$

$$C3: M_j > N_j, \quad \forall j = 1, 2, ..., J,$$

$$C4: \sum_{j=1}^{J} M_j = M, \quad \sum_{j=1}^{J} N_j = N.$$

IV. DISTRIBUTED PARTICLE SWARM OPTIMIZATION AIDED SOLUTION

A. Analysis and Simplification

Considering the homogeneity of the drones, Eq. (17) can be rewritten as:

$$\eta(A, B) = \sum_{j=1}^{J} \frac{\sum_{n=1}^{N_j} T_j C_n(R)}{M_j \int_0^{T_j^d} P_j(t)dt} \cdot \frac{M_j \int_0^{T_j^d} P_j(t)dt}{\sum_{j=1}^{J} M_j W} \triangleq \sum_{j=1}^{J} \eta_j \delta_j, \quad (19)$$

where $\eta_j \triangleq \frac{\sum_{n=1}^{N_j} T_j C_n(R)}{M_j \int_0^{T_j^d} P_j(t)dt}$ represents the specific energy

efficiency of the j-th flight circle, while $\delta_j \triangleq \frac{M_j \int_0^{T_j^d} P_j(t)dt}{\sum_{j=1}^{J} M_j W}$ denotes the j-th flight circle's energy consumption ratio against the system's total energy. Moreover, it may be readily inferred that we have $T_j = M_j T_j^h$ in (15), when η reaches its maximum value. Let us define the energy consumed by a UAV in the j-th flight circle as $W_j \triangleq \int_0^{T_j^d} P_j(t)dt$. Furthermore, we

have:

$$\eta_j = \frac{M_j T_j^h \sum_{n=1}^{N_j} C_n(R)}{M_j W_j} = \frac{T_j^h \sum_{n=1}^{N_j} C_n(R)}{W_j}, \quad (20)$$

$$\delta_j = \frac{M_j W_j}{MW}, \quad (21)$$

where $\sum_{j=1}^{J} \delta_j = 1, 0 < \delta_j \leq 1$. Upon combining Eq. (13) and Eq. (20), we arrive at:

$$\eta_j = \frac{\left(W_j - \frac{D_j}{V_t} P_t - P_a \frac{H}{V_a} - P_d \frac{H}{V_d}\right) \sum_{n=1}^{N_j} C_n(R)}{N_j P_h W_j}, \quad (22)$$

where $D_j = \sum_{k=1}^{N_j+1} d_{j,k}$.

It can be readily seen that $\frac{\partial \eta_j}{\partial W_j} > 0$ and $\frac{\partial \delta_j}{\partial W_j} > 0$. Hence, for the sake of maximizing $\eta(A, B)$, we have to satisfy:

$$W_j = W, \forall j = 1, 2, ..., J. \quad (23)$$

Furthermore, upon relying on Eq. (13), Eq. (15) and Eq. (23), we obtain:

$$T_j^h = \frac{W - P_a \frac{H}{V_a} - P_d \frac{H}{V_d} - P_t \frac{D_j}{V_t}}{N_j P_h}, j = 1, 2, ..., J, \quad (24)$$

as well as:

$$M_j = \left\lceil N_j \left(\frac{P_h \frac{D_j}{V_t} + P_h T_{home}}{W - P_a \frac{H}{V_a} - P_d \frac{H}{V_d} - P_t \frac{D_j}{V_t}} + 1 \right) \right\rceil, \ j = 1, 2, ..., J, \quad (25)$$

where $\lceil \cdot \rceil$ is the ceiling function representing the upper integer value. Moreover, Eq. (25) satisfies the constraint of $C3$ in the optimization problem $P1$. In practice, we can adjust the charging duration of T_{charge}, which is a function of T_{home}, to realize the integer ceiling operation. Therefore, problem $P1$ can be reformulated as:

$$P2: \quad \max_{A,B} \eta(A, B) = \sum_{j=1}^{J} \eta_j \delta_j$$

$$\text{s.t.} \quad C1: M_j T_j^h \geq T_j > 0, \quad \forall j = 1, 2, ..., J, \quad (26)$$

$$C2: \sum_{j=1}^{J} M_j = M, \sum_{j=1}^{J} N_j = N,$$

where $\eta_j = T_j^h \sum_{n=1}^{N_j} C_n(R)/W$ and $\delta_j = M_j/M$.

B. Distributed-PSO Algorithm Design

PSO is a stochastic optimization algorithm, which is inspired by the swarming behavior of collective forging for food by birds, bees or fish. In a PSO algorithm, M particles fly in an n-dimensional solution space, where $\{X_m(l) = (x_{m,1}(l), x_{m,2}(l), ..., x_{m,n}(l)), m \in \{1, 2..., M\}\}$ represents the position of the m-th particle in the l-th iteration, while $\{V_m(l) = (v_{m,1}(l), v_{m,2}(l), ..., v_{m,n}(l)), m \in \{1, 2..., M\}\}$ represents the current velocity of the m-th particle. Assuming that the objective function of η is employed as the fitness function, each particle has a hitherto best position $\{P_m(l) = (p_{m,1}(l), p_{m,2}(l), ..., p_{m,n}(l)), m \in \{1, 2..., M\}\}$ associated with its hitherto best fitness value, while the current globally optimal position of all particles is expressed by

---

Algorithm 1 Distributed Particle Swarm Optimization Algorithm

input:
user distribution, number of target locations (N), location of charging station, UAV altitude (H), UAV coverage radius (R), propagation parameters ($\eta_{los}, \eta_{nlos}, a, b$), iteration numbers ($I_A, I_B = O_B * N$), particle numbers ($M_A, M_B$);
start:
Randomly initialize coordinates of N target locations (strategy A) as $A^*(0)$;
Initialize strategy B as $B^*(0)$ of N flight circles;
Initialize iteration count: $k = 1$;
repeat
Stage-A start:
    Save current best strategy A: $X_1^A = A^*(k-1)$;
    Randomly generate rest particles' position:$X_m^A(m \neq 1)$;
    Randomly generate particles' velocity: V_m^A;
    Calculate each particle's fitness value according to Eq. (17): $F_A(X_m^A) \triangleq \eta(X_m^A, B^*(k-1))$, and get current P_m^A and P_g^A;
    while $l < I_A$ **do**
        Update velocity V_m^A and particles' position X_m^A according to Eq. (27);
        Update each particles' private best position P_m^A;
        Update global best position P_g^A;
    end while
    Update best strategy A: $A^*(k) = P_g^A$;
Stage-A end;
Stage-B start:
    Save current best strategy B: $X_1^B = B^*(k-1)$;
    Randomly generate rest particles' position:$X_m^B(m \neq 1)$;
    Randomly generate particles' velocity: V_m^B;
    Discrete X_m^B according to Eq. (28);
    Calculate each particle's fitness value according to Eq. (17): $F_B(X_m^B) \triangleq \eta(A^*(k), X_m^B)$, and get current P_m^B and P_g^B;
    while $l < I_B$ **do**
        Update particles' velocity V_m^B and position X_m^B according to Eq. (27);
        Discrete X_m^B according to Eq. (28);
        Update each particles' private best position P_m^B;
        Update global best position P_g^B;
    end while
    Update best strategy B: $B^*(k) = P_g^B$;
Stage-B end;
    Update k = k+1;
until The fractional increase of the objective value over L_s iterations is below the threshold $\epsilon_g > 0$;
output:
Optimal strategy A and Optimal strategy B: A^*, B^*.

$\{P_g(l) = (p_{g,1}(l), p_{g,2}(l), ..., p_{g,n}(l))\}$. In order to converge to the globally optimal position, the update functions of the velocities $\{V_m, m \in \{1, 2..., M\}\}$ as well as the positions

$\{X_m, m \in \{1, 2..., M\}\}$ are formulated as:

$$\begin{cases} V_m(l+1) = wV_m(l) + c_1\zeta_1(P_m(l) - X_m(l)) \\ \qquad\qquad + c_2\zeta_2(P_g(l) - X_m(l)), m \in \{1, 2..., M\}, \\ X_m(l+1) = X_m(l) + V_m(l+1), m \in \{1, 2..., M\}, \end{cases}$$
$$(27)$$

where w is the so-called inertia coefficient, while c_1 and c_2 represent the influence of the hitherto best position and the globally optimal position, respectively. Finally, ζ_1 and ζ_2 are a pair of random coefficients.

For solving problem $P2$ in Eq. (26), we propose a two-stage joint optimization algorithm termed as the distributed-PSO algorithm for the UAV deployment and CRRS problem. First of all, given the fixed N-location deployment strategy A, the capacity $C_n(R), n = 1, 2, ..., N$ within each service circle area can be determined. Then, problem (26) reduces to a single-strategy optimization problem in terms of $B = \{J, N_j, M_j\}$. Furthermore, when relying on Eq. (22) to Eq. (25), minimizing D_j yields the maximization of η_j. Let us define the shortest D_j of j-th flight circle as $D_{min,j}$, where $D_{min,j}$ and N_j in each flight circle can be calculated for a specific assignment strategy of the N target locations, respectively. Given that η_j is a function of both $D_{min,j}$ and N_j, the single-strategy optimization problem considered can be viewed as a generalized assignment problem, which is NP-hard. We can use a powerful discrete particle swarm optimization (DPSO) algorithm for finding a near-optimal solution of the CRRS strategy given a fixed A, say $B^* = \{J^*, N_j^*, M_j^*\}$. We define this stage as stage-B. On the other hand, when the strategy $B = \{J, N_j, M_j\}$ is given, the problem $P2$ becomes a so-called point deployment problem, which is a kind of facility location problems and is NP-hard. Hence, we apply the PSO algorithm for finding a near-optimal deployment strategy A^*. We name this stage as stage-A. Upon invoking a sufficiently high number of iterations, we arrive at a near-optimal strategy $\{A^*, B^*\}$ of the joint UAV deployment and UAV recharging and reshuffling problem.

Algorithm 1 summarizes the flow of our proposed distributed-PSO algorithm. In the algorithm, $A^*(k)$ and $B^*(k)$ represent the current optimal strategy A^* and B^* in the k-th iteration. Each iteration in the external loop includes two stages, namely stage-A and stage-B. Specifically, stage-A is composed by a PSO relying on I_A number of iterations, while stage-B represents a DPSO having I_B number of iterations. The algorithm ends when the fractional increase of the objective function value over L_s iterations is below the threshold $\epsilon_g > 0$. The details of the two stages are described as follows.

1) Stage-A: The objective of stage-A is to find a near-optimal strategy A in conjunction with a given fixed CRRS strategy B, which can be initialized or be calculated by the iterative result of stage-B. We use the PSO algorithm for optimizing strategy A, where $X_m^A = (x_{m,1}^A, x_{m,2}^A, ..., x_{m,N}^A)$ is defined as a N-dimensional variable. Moreover, $x_{m,n}^A = (x_{m,n}, y_{m,n})$ in X_m^A represents the horizontal coordinate of the n-th target location of the m-th particle, where we have $m \in \{1, 2, ..., M_A\}$, with M_A representing the number of PSO particles at this stage. Furthermore, the fitness function of the PSO is η in Eq. (26).

2) Stage-B: The objective of stage-B is to optimize the CRRS strategy B, while the fixed A is either the original strategy or it is the one calculated by the iterative result of stage-A. However, the objective function is actually equivalent to that of an optimal assignment problem allocating N target locations to a total of J flight circles. In order to find the optimum relying on the DPSO algorithm, we define $X_m^B = (x_{m,1}^B, x_{m,2}^B, ..., x_{m,N}^B)$ as an N-dimensional variable, where $x_{m,n}^B = j$ ($j \in \{1, 2, ..., J\}$) indicates that the n-th target location is assigned to the j-th flight circle. Furthermore, considering the integer nature of X_m^B in our DPSO algorithm, we discretize X_m^B in Eq. (27), and use the ceiling function:

$$X_{m,l}^B = \lceil X_{m,l}^B \rceil. \qquad (28)$$

Additionally, considering that the choice of N may affect the convergence efficiency, the number of iterations is set to $I_B = O_B \cdot N$, where O_B represents a scaling factor. Moreover, the fitness function of the DPSO is η in Eq. (26).

C. Algorithmic Convergence Analysis

The proposed Algorithm 1 has two stages, i.e. stage-A and stage-B, which are reminiscent of block coordinate descent methods, where each stage can be viewed as a block. In the algorithm, strategy A and strategy B are alternately optimized, while always fixing the other strategy. Moreover, the strategies obtained in the current iteration are the input of the next iteration. In Algorithm 1, each stage adopts the PSO method, yielding a near-optimal solution. Hence, the convergence of Algorithm 1 cannot be directly analyzed by the classical block coordinate descent method, which can be proved as follows.

In stage-A, the current optimal strategy $A^*(k-1)$ obtained in the previous iteration is saved in the initial particles of the PSO algorithm. As for the convergence properties of the PSO algorithm, given fixed $B^*(k-1)$, we have:

$$\eta[A^*(k-1), B^*(k-1)] \leq \eta[A^*(k), B^*(k-1)]. \qquad (29)$$

Similarly, in stage-B, given fixed $A^*(k)$, $B^*(k-1)$ follows:

$$\eta[A^*(k), B^*(k-1)] \leq \eta[A^*(k), B^*(k)]. \qquad (30)$$

Hence, based on Eq. (29) and Eq. (30), we have:

$$\eta[A^*(k-1), B^*(k-1)] \leq \eta[A^*(k), B^*(k)]. \qquad (31)$$

Eq. (31) points out that the objective function value of Eq. (26) is non-decreasing in each iteration. Since η is upper bounded by a finite value, the convergence of Algorithm 1 is guaranteed. Given that the PSO algorithm in stage-A and the DPSO algorithm in stage-B are re-initialized in each iteration, the proposed Algorithm 1 is capable of avoiding local optima. Hence, Algorithm 1 closely approximates the optimal value, even if the PSO algorithm and DPSO algorithm normally arriving at a sub-optimal solution.

D. Algorithmic Complexity Analysis

The complexity order of the distributed-PSO algorithm can be estimated as:

$$O\left(I_g \cdot [(I_A \cdot M_A \cdot T_A) + (I_B \cdot M_B \cdot T_B)]\right), \qquad (32)$$

TABLE II
SIMULATION PARAMETERS [10], [37]

Parameters	Values
Channel parameters $(\eta_{los}, \eta_{nlos}, a, b)$	(1,20,9.61,0.61)
Carrier frequency (f)	2.4 GHz
Bandwidth (B)	1 MHz
Variance of noise (σ^2)	5×10^{-15} W/Hz
UAV transmit power (P_{tr})	0.5 W
UAV's altitude (H)	100 m
UAV's coverage radius (R)	100 m
UAV's hovering power (P_h)	200 W
UAV's flying power/speed (P_t/V_t)	240 W / 10 m/s
UAV's ascending power/speed (P_a/V_a)	250 W / 5 m/s
UAV's descending power/speed (P_d/V_d)	180 W / 5 m/s
UAV's battery capacity (W)	97.58 Wh
Charging duration (T_{charge})	5 min⋆

⋆ In reality, we can replace the battery of drones for achieving a sharp reduction in charging duration.

TABLE III
PARAMETERS OF DISTRIBUTED-PSO ALGORITHM

Parameters	Values
L_s, ϵ_g	10, 10^{-4}
Stage-A (I_A, M_A, c_1, c_2, w)	(100, 100, 1.49 , 1.49, 0.729)
Stage-B (O_B, M_B, c_1, c_2, w)	(20, 50, 1.49, 1.49, 0.729)

where T_A and T_B represent each particles' operation time in the PSO algorithm of stage-A and stage-B respectively, while I_g is the number of iterations in the external loop of Algorithm 1. Since the number of dimensions of the particles defined as $X_m^A = (x_{m,1}^A, x_{m,2}^A, ..., x_{m,N}^A)$ in stage-A equals to the number of the target locations (N), T_A linearly increases with the number N. Similarly, T_B linearly increases with N. Moreover, we have $I_B = O_B \cdot N$. Hence, the complexity of Algorithm 1 can be expressed as $T(N) = O(N^2)$, which obeys a polynomial complexity order.

V. SIMULATION RESULTS

In our simulations, we consider a 500×500 m rectangular area, where the users are distributed following the Poissonian clustering process. The center of the rectangular service area is located at the origin $[0,0]$. The essential parameters are summarized in Table. II [10], where some of the UAV parameters are those of the drone Matrice 100 produced by DJI [37]. Table. III shows the parameters of distributed-PSO algorithm. The numerical simulations are developed by using MATLAB R2017a.

Fig. 4 shows the energy efficiency η versus the X-coordinate of the charging station $(y = 0)$, parameterized by the total number of target service locations N. Observe from the figure that the communication energy efficiency near-linearly decreases with the distance between the origin $[0,0]$ and the charging station. Explicitly, since $T_j = M_j T_j^h$ as well as bearing in mind Eq. (17), the energy efficiency η is a linear function of the hovering duration T_j^h, that is in turn a near-linear function of the distance of the charging station from the area center according to Eq. (24). Hence, the distance between the charging station and the center of the service area imposes
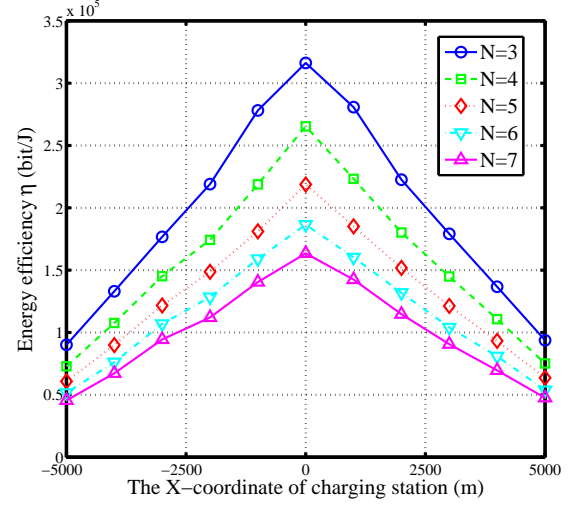

Fig. 4. Energy efficiency η versus the position of the charging station parameterized by the total number of target service locations N.
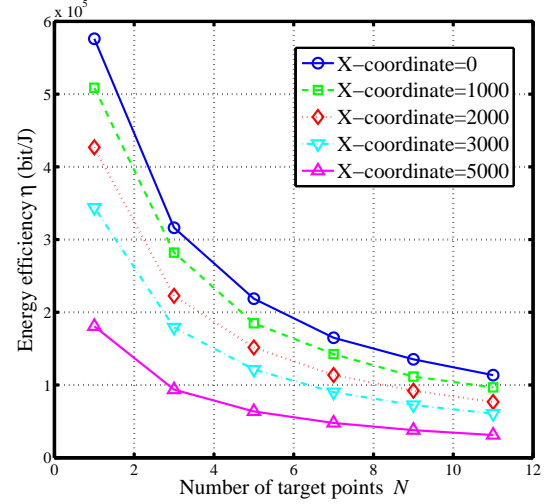

Fig. 5. Energy efficiency η versus the number of target points parameterized by the X-coordinate of charging station.

a substantial impact on the deployment and cyclic recharging of the UAVs. Moreover, when the number of target service points N is increased, the energy efficiency is degraded. This is because the target service areas may overlap, which results in an energy efficiency reduction.

The performance of the energy efficiency η versus the number N of target points is portrayed in Fig. 5, where we can see that the energy efficiency η is reduced as a function of the number of target points. Moreover, the larger the number of target points, the more slowly the rate decreases, which is a consequence of the linear relationship between the energy efficiency η and the hovering duration T_j^h as well as the reciprocal relationship between T_j^h and N_j in Eq. (24). As shown in Fig. 5, the curve associated with the scenario, when the X-coordinate of the charging station is 5000m is more flat than those of the others, which implies that the influence of the
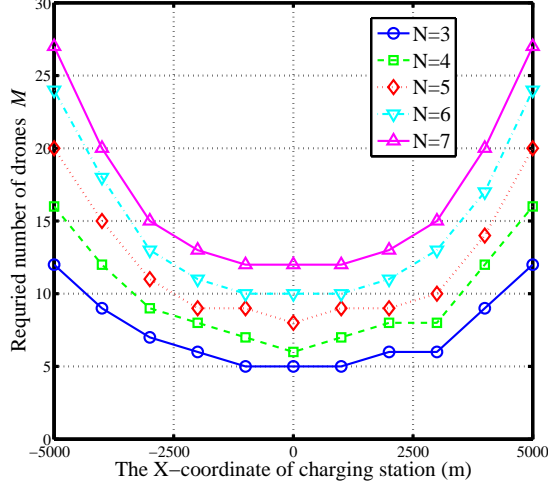
Fig. 6. Required number of drones M versus the position of the charging station parameterized by the total number of target service locations N.
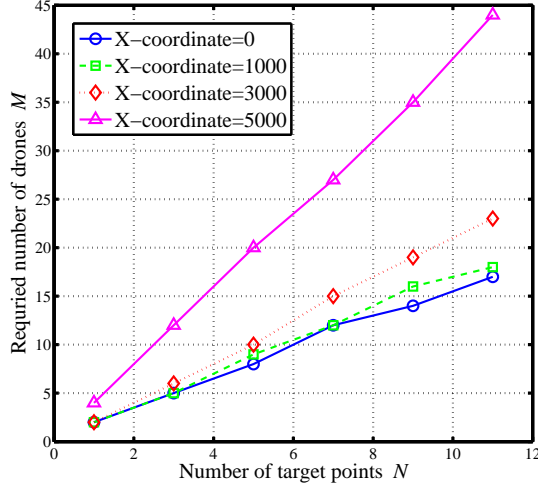

Fig. 8. The performance benefits of iterations and an example of the UAV deployment and CRRS associated with $N = 5$, $M = 9$ and $J = 3$.

Fig. 7. Required number of drones M versus the number of target points parameterized by the X-coordinate of charging station.

Fig. 9. Convergence analysis with different parameters at the condition of $N = 3$, X-coordinate $= 500$.

number of target points N on the energy efficiency η reduces, when the charging station is farther away from the origin.

Fig. 6 illustrates the influence of the total number of drones required, namely M versus the X-coordinate of the charging station, where the Y-coordinate is fixed. The figure shows that the required number of drones M non-linearly increases when the charging station is located far away from the origin $[0, 0]$. More explicitly, having a long distance between the charging station and the service area results in a short hovering duration for the UAV, which determines the longest affordable reshuffling interval of the UAVs in each flight cycle and can be corroborated by Eq. (24) and Eq. (25). Therefore, in order to guarantee that each target point is supported by a hovering UAV at any moment, more UAVs are needed.

Fig. 7 shows the required number of drones M versus the number of target points parameterized by the X-coordinate of
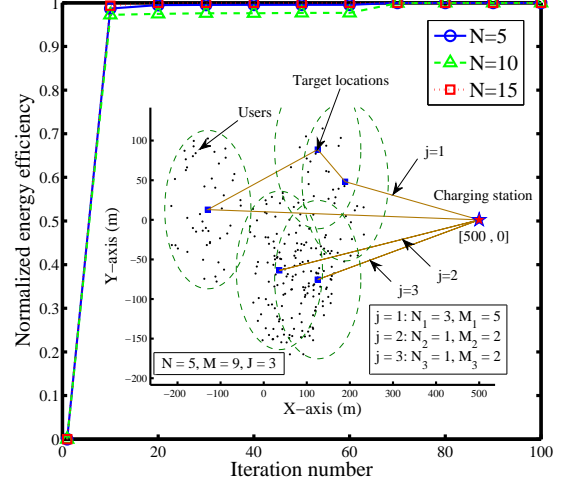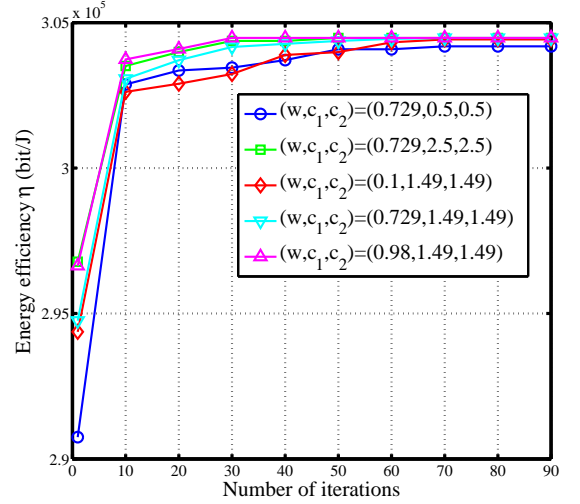
the charging station. The required number of UAVs M linearly increases with the number N of target points. Furthermore, the slope of the curves M becomes steeper as the distance between the coverage area center and the charging station becomes longer.

Fig. 8 portrays the iterative performance improvement of our proposed optimization algorithms, indicating that convergence is attained after about 70 iterations. Moreover, the sub-figure in Fig. 8 provides an example of near-optimal results for the UAV deployment as well as for the CRRS strategy, where the blue dots show the target locations used, while the brown lines indicate the flight paths of UAVs. Finally, the red star shows the location of charging station. Explicitly, given a fixed charging station location of [500, 0] and a total of $N = 5$ target service locations, we arrive at the optimal UAV deployment strategy A^* associated with the
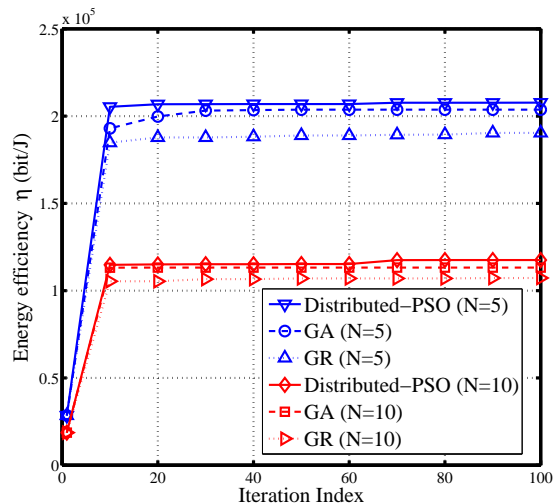
Fig. 10. The energy efficiency performance comparison among Distributed-PSO, GA and GR.

optimizing the energy-efficiency of multi-UAV communication systems with the goal of providing seamless long-term coverage in urban areas. Firstly, we introduced a novel UAV energy consumption model and defined our energy-efficiency objective function. Secondly, our energy-efficient rechargeable UAV deployment strategy was optimized under the constraint of providing seamless coverage. Thirdly, relying on PSO, we designed a two-stage joint optimization algorithm for finding the near optimal deployment strategy as well as UAV CRRS. Finally, Our simulation results have confirmed the convergence of the two-stage joint optimization algorithm.

coordinates of $[-129.7, 12.91]$, $[125.4, 88.67]$, $[189.1, 48.11]$, $[36.38, -63.86]$ and $[125.4, -75.45]$, respectively. Furthermore, as for the optimal UAV CRRS B^*, a total of $J^* = 3$ independent flight route circles and $M^* = 9$ UAVs are required for covering all the 5 target locations within each flight route circle associated with $N_1 = 3, M_1 = 5, N_2 = 1, M_2 = 2$ and $N_3 = 1, M_3 = 2$, respectively.

Fig. 9 illustrates the convergence of the proposed algorithm associated with various PSO and DPSO parameters, where w, c_1 and c_2 are set to the same values for the PSO and DPSO. The figure portrays that the change of parameters has little effect on the convergence of the algorithm, while the parameters fall into the convergence area [38]. Furthermore, the objective function values associated with various parameters all converge to a similar value, which verifies the convergence of the proposed algorithm.

For benchmarking the performance of the proposed algorithm, we opt for the classic Genetic Algorithm (GA) and the classic Greedy Algorithm (GR) for both stage-A and stage-B in Algorithm 1. In the GA, the population sizes and generation numbers are the same as the particle numbers and the iteration numbers of the PSO and DPSO in Algorithm 1, while the crossover probability and the mutation probability of GA are set as $P_c = 0.8$ and $P_m = 0.1$, respectively. Fig. 10 contrasts our results, where the position of the charging station is set to $(500, 0)$. Observe from Fig. 10 that the distributed-PSO algorithm converges faster than both the GA and GR in the context of both $N = 5$ and $N = 10$, which is because the search trajectory of PSO is better guided than that of the GA and GR as a benefit of its memory. Recall that the energy efficiency of $N = 5$ is much higher than that of $N = 10$, which is also seen in Fig. 5.

VI. CONCLUSIONS

Providing seamless long-term coverage in emergency situations is of vital importance. In this paper, we aimed for

REFERENCES

[1] J. Wang, C. Jiang, Z. Han, Y. Ren, R. G. Maunder, and L. Hanzo, "Taking drones to the next level: Cooperative distributed unmanned-aerial-vehicular networks for small and mini drones," *IEEE Vehicular Technology Magazine*, vol. 12, no. 3, pp. 73–82, Mar. 2017.
[2] F. Cheng, S. Zhang, Z. Li, Y. Chen, N. Zhao, R. Yu, and V. C. M. Leung, "UAV trajectory optimization for data offloading at the edge of multiple cells," *IEEE Transactions on Vehicular Technology*, vol. 67, no. 7, pp. 6732–6736, Mar. 2018.
[3] S. Jeong, O. Simeone, and J. Kang, "Mobile edge computing via a UAV-mounted cloudlet: Optimization of bit allocation and path planning," *IEEE Transactions on Vehicular Technology*, vol. 67, no. 3, pp. 2049–2063, May 2017.
[4] X. Yuan, Z. Feng, W. Xu, W. Ni, A. Zhang, Z. Wei, and R. P. Liu, "Capacity analysis of UAV communications: Cases of random trajectories," *IEEE Transactions on Vehicular Technology*, vol. 67, no. 8, pp. 7564–7576, Apr. 2018.
[5] L. Xiao, X. Lu, D. Xu, Y. Tang, L. Wang, and W. Zhuang, "UAV relay in VANETs against smart jamming with reinforcement learning," *IEEE Transactions on Vehicular Technology*, vol. 67, no. 5, pp. 4087–4097, Jan. 2018.
[6] L. Gupta, R. Jain, and G. Vaszkun, "Survey of important issues in UAV communication networks," *IEEE Communications Surveys & Tutorials*, vol. 18, no. 2, pp. 1123–1152, Feb. 2016.
[7] J. Zhang, T. Chen, S. Zhong, J. Wang, W. Zhang, X. Zuo, R. G. Maunder, and L. Hanzo, "Aeronautical Ad Hoc networking for the internet-above-the-clouds," *Proceedings of the IEEE*, vol. 107, no. 5, pp. 868–911, May 2019.
[8] M. Alzenad, A. El-Keyi, F. Lagum, and H. Yanikomeroglu, "3D placement of an unmanned aerial vehicle base station (UAV-BS) for energy-efficient maximal coverage," *IEEE Wireless Communications Letters*, vol. 6, no. 4, pp. 434–437, Aug. 2017.
[9] M. Mozaffari, W. Saad, M. Bennis, and M. Debbah, "Wireless communication using unmanned aerial vehicles (UAVs): Optimal transport theory for hover time optimization," *IEEE Transactions on Wireless Communications*, vol. 16, no. 12, pp. 8052–8066, Dec. 2017.
[10] J. Lu, S. Wan, X. Chen, Z. Chena, P. Fan, and K. B. Letaief, "Beyond empirical models: Pattern formation driven placement of UAV base stations," *IEEE Transactions on Wireless Communications*, vol. 17, no. 6, pp. 3641–3655, Jun. 2018.
[11] Y. Zeng and R. Zhang, "Energy-efficient UAV communication with trajectory optimization," *IEEE Transactions on Wireless Communications*, vol. 16, no. 6, pp. 3747–3760, Jun. 2017.
[12] D. Yang, Q. Wu, Y. Zeng, and R. Zhang, "Energy trade-off in ground-to-UAV communication via trajectory design," *IEEE Transactions on Vehicular Technology*, vol. 67, no. 7, pp. 6721–6726, Jul. 2018.
[13] M. Hua, Y. Wang, Z. Zhang, C. Li, Y. Huang, and L. Yang, "Power-efficient communication in UAV-aided wireless sensor networks," *IEEE Communications Letters*, vol. 22, no. 6, pp. 1264–1267, Apr. 2018.
[14] C. D. Franco and G. C. Buttazzo, "Energy-aware coverage path planning of UAVs," in *IEEE International Conference on Autonomous Robot Systems and Competitions*, Vila Real, Portugal, May 2015, pp. 111–117.
[15] J. Wang, C. Jiang, Z. Wei, C. Pan, H. Zhang, and Y. Ren, "Joint UAV hovering altitude and power control for space-air-ground IoT networks," *IEEE Internet of Things Journal*, vol. 6, no. 2, pp. 1741–1753, Apr. 2019.
[16] Y. Zeng, R. Zhang, and J. L. Teng, "Wireless communications with unmanned aerial vehicles: Opportunities and challenges," *IEEE Communications Magazine*, vol. 54, no. 5, pp. 36–42, May 2016.

[17] R. Duan, J. Wang, C. Jiang, Y. Ren, and L. Hanzo, "The transmit-energy vs computation-delay trade-off in gateway-selection for heterogenous cloud aided multi-UAV systems," *IEEE Transactions on Communications*, vol. 67, no. 4, pp. 3026–3039, Apr. 2019.

[18] A. Hourani, S. Kandeepan, and S. Lardner, "Optimal LAP altitude for maximum coverage," *IEEE Wireless Communications Letters*, vol. 3, no. 6, pp. 569–572, Jul. 2014.

[19] M. Mozaffari, W. Saad, M. Bennis, and M. Debbah, "Drone small cells in the clouds: Design, deployment and performance analysis," in *IEEE Global Communications Conference (GLOBECOM)*, San Diego, CA, Dec. 2015, pp. 1–6.

[20] M. Alzenad, A. El-Keyi, and H. Yanikomeroglu, "3D placement of an unmanned aerial vehicle base station for maximum coverage of users with different QoS requirements," *IEEE Wireless Communications Letters*, vol. 7, no. 1, pp. 38–41, Sep. 2017.

[21] R. I. B. Yaliniz, A. El-Keyi, and H. Yanikomeroglu, "Efficient 3-D placement of an aerial base station in next generation cellular networks," in *IEEE International Conference on Communications (ICC)*, Kuala Lumpur, Malaysia, May 2016, pp. 1–5.

[22] F. Z. Tao Zhang, P. Y. Lei Feng, B. R. Wenjing Li, and H. Rutagemwa, "Capacity enhancement for next generation mobile networks using mmWave aerial base station," in *IEEE Global Communications Conference (GLOBECOM)*, Singapore, Dec. 2017, pp. 1–6.

[23] X. Zhang and L. Duan, "Fast deployment of UAV networks for optimal wireless coverage," *IEEE Transactions on Mobile Computing*, vol. 18, no. 3, pp. 588–601, Mar. 2019.

[24] J. Lyu, Y. Zeng, R. Zhang, and J. L. Teng, "Placement optimization of UAV-mounted mobile base stations," *IEEE Communications Letters*, vol. 21, no. 3, pp. 604–607, Nov. 2016.

[25] M. Mozaffari, W. Saad, M. Bennis, and M. Debbah, "Efficient deployment of multiple unmanned aerial vehicles for optimal wireless coverage," *IEEE Communications Letters*, vol. 20, no. 8, pp. 1647–1650, Jun. 2016.

[26] ——, "Unmanned aerial vehicle with underlaid device-to-device communications: Performance and tradeoffs," *IEEE Transactions on Wireless Communications*, vol. 15, no. 6, pp. 3949–3963, Feb. 2016.

[27] J. Lyu, Y. Zeng, and R. Zhang, "UAV-aided offloading for cellular hotspot," *IEEE Transactions on Wireless Communications*, vol. 17, no. 6, pp. 3988–4001, Mar. 2018.

[28] K. Li, W. Ni, X. Wang, R. Liu, S. Kanhere, and S. Jha, "Energy-efficient cooperative relaying for unmanned aerial vehicles," *IEEE Transactions on Mobile Computing*, vol. 15, no. 6, pp. 1377–1386, Aug. 2015.

[29] J. Zhang, Y. Zeng, and R. Zhang, "Spectrum and energy efficiency maximization in UAV-enabled mobile relaying," in *IEEE International Conference on Communications*, Paris, France, Jul. 2017, pp. 1–6.

[30] J. Chen and D. Gesbert, "Optimal positioning of flying relays for wireless networks: A LOS map approach," in *IEEE International Conference on Communications*, Paris, France, Jul. 2017, pp. 1–6.

[31] M. Mozaffari, W. Saad, M. Bennis, and M. Debbah, "Mobile unmanned aerial vehicles (UAVs) for energy-efficient Internet of things communications," *IEEE Transactions on Wireless Communications*, vol. 16, no. 11, pp. 7574–7589, Sep. 2017.

[32] Y. Bouzid, Y. Bestaoui, and H. Siguerdidjane, "Quadrotor-UAV optimal coverage path planning in cluttered environment with a limited onboard energy," in *IEEE/RSJ International Conference on Intelligent Robots and Systems (IROS)*, Vancouver, Canada, Sep. 2017, pp. 979–984.

[33] L. Wang, B. Hu, and S. Chen, "Energy efficient placement of a drone base station for minimum required transmit power," *IEEE Wireless Communications Letters, DOI: 10.1109/LWC.2018.2808957*, pp. 1–4, Feb. 2018.

[34] J. Yu, R. Zhang, Y. Gao, and L. L. Yang, "Modularity-based dynamic clustering for energy efficient UAVs aided communications," *IEEE Wireless Communications Letters*, vol. 7, no. 5, pp. 728–731, Mar. 2018.

[35] M. D. F. Angelo Trotta and L. B. Kaushik R. Chowdhury, "Fly and recharge: Achieving persistent coverage using small unmanned aerial vehicles (SUAVs)," in *IEEE International Conference on Communications (ICC)*, Paris, France, May 2017, pp. 1–7.

[36] Z. Liu, R. Sengupta, and A. Kurzhanskiy, "A power consumption model for multi-rotor small unmanned aircraft systems," in *International Conference on Unmanned Aircraft Systems (ICUAS)*, Miami, FL, USA, Jun. 2017, pp. 310–315.

[37] DJI Inc., "Technical parameters of DJI Matrice 100," http://www.dji.com/cn/matrice100/info#specs, online; accessed 4th August, 2018.

[38] M. Jiang, Y. P. Luo, and S. Y. Yang, "Stochastic convergence analysis and parameter selection of the standard particle swarm optimization algorithm," *Information Processing Letters*, vol. 102, no. 1, pp. 8–16, Apr. 2007.

Xiaowei Li received the B.S. degree in Communication Engineering from North University of China, Taiyuan, in 2007, and the M.S. degree in Instrument Science and Technology from Beijing University of Technology, Beijing, in 2012. He is currently pursuing the Ph.D. degree with the Beijing Advanced Innovation Center for Future Internet Technology in Beijing University of Technology. His main research interests include the UAV communications and mobile wireless networks.

Haipeng Yao (M'16) is an Associate Professor in Beijing University of Posts and Telecommunications. Haipeng Yao received his Ph.D. in the Department of Telecommunication Engineering at University of Beijing University of Posts and Telecommunications in 2011. He has been engaged in research on future internet architecture, network AI, Big Data, cognitive radio networks, and optimization of protocols and architectures for broadband wireless networks. He has published more than 80 papers in prestigious peer-reviewed journals and conferences.

Jingjing Wang (S'14-M'19) received his B.S. degree in Electronic Information Engineering from Dalian University of Technology, Liaoning, China in 2014 and the Ph.D. degree in Information and Communication Engineering from Tsinghua University, Beijing, China in 2019, both with the highest honors. From 2017 to 2018, he visited the Next Generation Wireless Group chaired by Prof. Lajos Hanzo, University of Southampton, UK. Dr. Wang is currently a postdoc researcher at Department of Electronic Engineering, Tsinghua University. His research interests include resource allocation and network association, learning theory aided modeling, analysis and signal processing, as well as information diffusion theory for mobile wireless networks. Dr. Wang received China Postgraduate National Scholarship Award in 2017, Best Journal Paper Award from IEEE Technical Committee on Green Communications & Computing in 2018, Beijing Distinguished Graduated Student Award, Tsinghua Outstanding Distinguished Doctoral Dissertation, Best Paper Award from IEEE ICC in 2019.

Xiaobin Xu is a Lecturer at the Beijing University of Technology. He obtained his PhD at Beijing University of Posts and Telecommunications in 2014. He joined the Beijing University of Technology as a Lecturer with the Beijing Advanced Innovation Center for Future Internet Technology in 2017. His current research areas include data prediction algorithms for wireless sensor networks, routing algorithms for space-terrestrial integrated networks.
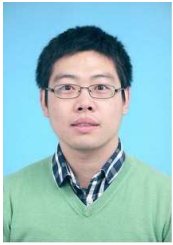
Chunxiao Jiang (S'09-M'13-SM'15) received the B.S. degree from Beihang University, Beijing in 2008 and the Ph.D. degree in electronic engineering from Tsinghua University, Beijing in 2013, both with the highest honors. From 2011 to 2012, he visited University of Maryland, College Park as a joint PhD supported by China Scholarship Council. From 2013 to 2016, he was a postdoc with Tsinghua University, during which he visited University of Maryland, College Park and University of Southampton. Since July 2016, he became an assistant professor in Tsinghua Space Center, Tsinghua University. His research interests include space networks and heterogeneous networks. Dr. Jiang is the recipient of the Best Paper Award from IEEE GLOBECOM in 2013, the Best Student Paper Award from IEEE GlobalSIP in 2015, IEEE Communications Society Young Author Best Paper Award in 2017, the Best Paper Award IWCMC in 2017, the Best Journal Paper Award of IEEE ComSoc Technical Committee on Communications Systems Integration and Modeling 2018.

Lajos Hanzo (F'04) FREng, FIET, Fellow of EURASIP, received his 5-year degree in electronics in 1976 and his doctorate in 1983 from the Technical University of Budapest. In 2009 he was awarded an honorary doctorate by the Technical University of Budapest and in 2015 by the University of Edinburgh. In 2016 he was admitted to the Hungarian Academy of Science. During his 40-year career in telecommunications he has held various research and academic posts in Hungary, Germany and the UK. Since 1986 he has been with the School of Electronics and Computer Science, University of Southampton, UK, where he holds the chair in telecommunications. He has successfully supervised 119 PhD students, co-authored 18 John Wiley/IEEE Press books on mobile radio communications totalling in excess of 10 000 pages, published 1800+ research contributions at IEEE Xplore, acted both as TPC and General Chair of IEEE conferences, presented keynote lectures and has been awarded a number of distinctions. Currently he is directing a 60-strong academic research team, working on a range of research projects in the field of wireless multimedia communications sponsored by industry, the Engineering and Physical Sciences Research Council (EPSRC) UK, the European Research Council's Advanced Fellow Grant and the Royal Society's Wolfson Research Merit Award. He is an enthusiastic supporter of industrial and academic liaison and he offers a range of industrial courses. He is also a Governor of the IEEE ComSoc and VTS. He is a former Editor-in-Chief of the IEEE Press and a former Chaired Professor also at Tsinghua University, Beijing. For further information on research in progress and associated publications please refer to http://www-mobile.ecs.soton.ac.uk.